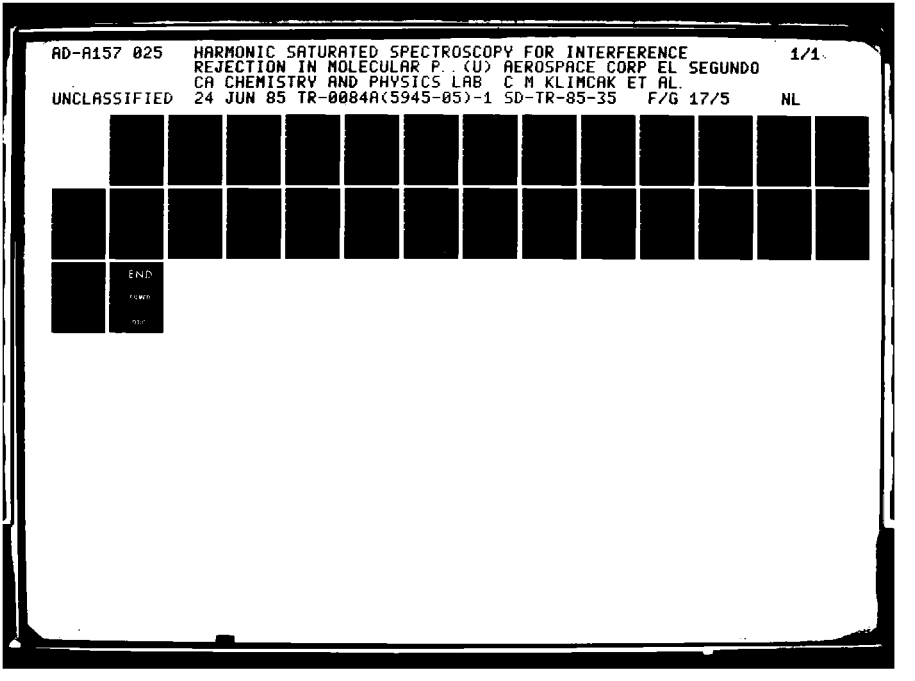
AD-A157 025 HARMONIC SATURATED SPECTROSCOPY FOR INTERFERENCE 1/1
REJECTION IN MOLECULAR P.. (U) AEROSPACE CORP EL SEGUNDO
CA CHEMISTRY AND PHYSICS LAB C M KLIMCAK ET AL.
UNCLASSIFIED 24 JUN 85 TR-0084A(5945-05)-1 SD-TR-85-35 F/G 17/5 NL
END
FILMED
DTIC

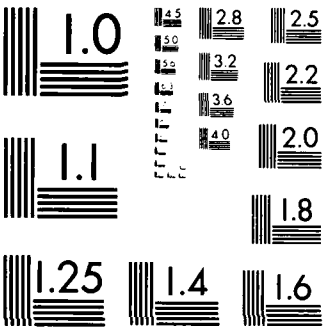

REPORT SD-TR-85-35

Harmonic Saturated Spectroscopy for Interference Rejection in Molecular Photoacoustic Infrared Detection

C. M. KLIMCAK and J. A. GELBWACHS
Chemistry and Physics Laboratory
Laboratory Operations
The Aerospace Corporation
El Segundo, CA 90245

24 June 1985

Prepared for
SPACE DIVISION
AIR FORCE SYSTEMS COMMAND
Los Angeles Air Force Station
P.O. Box 92960, Worldway Postal Center
Los Angeles, CA 90009-2960

This report was submitted by The Aerospace Corporation, El Segundo, CA 90245, under Contract No. F04701-83-C-0084 with the Space Division, P.O. Box 92960, Worldway Postal Center, Los Angeles, CA 90009. It was reviewed and approved for The Aerospace Corporation by S. Feuerstein, Director, Chemistry and Physics Laboratory.

Lt David Barnaby, SD/YNCS, was the project officer for the Mission-Oriented Investigation and Experimentation (MOIE) Program.

This report has been reviewed by the Public Affairs Office (PAS) and is releasable to the National Technical Information Service (NTIS). At NTIS, it will be available to the general public, including foreign nationals.

This technical report has been reviewed and is approved for publication. Publication of this report does not constitute Air Force approval of the report's findings or conclusions. It is published only for the exchange and stimulation of ideas.

David Barnaby

DAVID BARNABY, 1LT, USAF
MOIE Project Officer
SD/YNCS

Joseph Hess

JOSEPH HESS, GM-15
Director, AFSTC West Coast Office
AFSTC/WCO OL-AB

UNCLASSIFIED

SECURITY CLASSIFICATION OF THIS PAGE *(When Data Entered)*

REPORT DOCUMENTATION PAGE		READ INSTRUCTIONS BEFORE COMPLETING FORM
1. REPORT NUMBER SD-TR-85-35	2. GOVT ACCESSION NO. AD. A157 625	3. RECIPIENT'S CATALOG NUMBER
4. TITLE *(and Subtitle)* HARMONIC SATURATED SPECTROSCOPY FOR INTERFERENCE REJECTION IN MOLECULAR PHOTOACOUSTIC INFRARED DETECTION		5. TYPE OF REPORT & PERIOD COVERED 6. PERFORMING ORG. REPORT NUMBER TR-0084A(5945-05)-1
7. AUTHOR(s) Charles M. Klimcak and Jerry A. Gelbwachs		8. CONTRACT OR GRANT NUMBER(s) F04701-83-C-0084
9. PERFORMING ORGANIZATION NAME AND ADDRESS The Aerospace Corporation El Segundo, Calif. 90245		10. PROGRAM ELEMENT, PROJECT, TASK AREA & WORK UNIT NUMBERS
11. CONTROLLING OFFICE NAME AND ADDRESS Space Division Los Angeles Air Force Station Los Angeles, Calif. 90009-2960		12. REPORT DATE 24 June 1985 13. NUMBER OF PAGES 25
14. MONITORING AGENCY NAME & ADDRESS *(If different from Controlling Office)*		15. SECURITY CLASS. *(of this report)* Unclassified 15a. DECLASSIFICATION/DOWNGRADING SCHEDULE

16. DISTRIBUTION STATEMENT *(of this Report)*

Approved for public release; distribution unlimited.

17. DISTRIBUTION STATEMENT *(of the abstract entered in Block 20, if different from Report)*

18. SUPPLEMENTARY NOTES

19. KEY WORDS *(Continue on reverse side if necessary and identify by block number)*

Infrared trace detection
Interference rejection
Molecular spectroscopy
Photoacoustic spectroscopy

20. ABSTRACT *(Continue on reverse side if necessary and identify by block number)*

The application of harmonic saturated spectroscopy to molecular detection in the infrared regime was investigated. Experimental measurements using SF_6 as a model gas were performed with a CO_2 laser photoacoustic molecular-vapor detector operating in the 9 through 11-μm portion of the infrared regime. These experiments demonstrated the negligible loss of absolute sensitivity, the maintenance of a characteristic readily identifiable absorption profile,

DD FORM 1473 (FACSIMILE)

UNCLASSIFIED

SECURITY CLASSIFICATION OF THIS PAGE *(When Data Entered)*

19. KEY WORDS (Continued)

20 ABSTRACT (Continued)

and the ability to scale with laser intensity under the proper conditions. Our work demonstrates the importance of a laser modulation waveform that is completely devoid of spatial asymmetries for the realization of the full potential of this method.

ACKNOWLEDGMENT

The authors wish to thank Dr. Gary Loper for originally suggesting this investigation.

CONTENTS

FIGURES

I. INTRODUCTION

Trace molecular detection is often limited by an interfering background signal that is much larger than the intrinsic noise-equivalent response of the detector. Consider, for example, molecular detection with a photoacoustic spectrophone operating in the infrared regime. Such instruments have nearly attained the theoretical noise-equivalent absorption detectivity of 10^{-10} cm^{-1} under controlled laboratory conditions.[1] This high sensitivity may not be achieved under realistic detection conditions because of the interfering background absorption of normal atmospheric constituents.

The source of background signals is not always restricted to atmospheric constituents. Absorption by the windows of the photoacoustic cell may also limit detectivity. The strength of this absorption response depends upon the quality and composition of the window material, and on the geometry of the photoacoustic cell. Even the highest-quality ZnSe substrates exhibit a residual window absorption of $\sim 10^{-3}$ cm^{-1}.

An improvement in the trace-vapor detectivity of a photoacoustic spectrophone could be achieved by employing a detection scheme that efficiently discriminates against these interferents. Harmonic saturated spectroscopy has been shown in the past to provide greatly enhanced discrimination against Mie scattering interferences in the optical regime.[2] We have implemented this technique in the infrared regime and applied it to the photoacoustic detection of trace vapors. In this technique, an optically saturated, nonlinear absorption response is generated by a symmetrically modulated light source of high intensity. The Fourier decomposition of this saturated response yields harmonic overtone responses that contain contributions from only the nonlinear components of the overall signal. Detection with a lock-in amplifier at the second harmonic of the laser modulation frequency theoretically permits rejection of the signal contributions from all linearly responding species in the gas mixture. Enhanced discrimination against an interferent is predicted whenever the interferent signal does not saturate as readily as the signal of the trace vapor of interest.

The suppression of the effect of a linearly responding background by harmonic analysis of saturated atomic fluorescence was first demonstrated by Frueholz and Gelbwachs.[2] Kreuzer, in his early formulation of the infrared photoacoustic effect, suggested employing this technique to reduce the effect of interferences arising from both far-wing contributions of an essentially "off-resonant" absorber, and from windows and cell walls.[3] However, no experimental data in the infrared have been published to date.

II. HARMONIC SATURATED SPECTROSCOPY

From the initial work of Frueholz and Gelbwachs,[2] the amplitude of the harmonic responses (a_n) of a simple, homogeneously broadened two-level system at any intensity (I) is given by

$$a_n = \frac{(1 - \alpha)}{(1 - \alpha^2)^{1/2}} \left[\frac{(1 - \alpha^2)^{1/2} - 1}{\alpha}\right]^n \qquad (n > 1) \tag{1}$$

where $\alpha = I/(2I_0 + I)$

and I_0 is the saturation intensity. For collisionally dominated relaxation, $I_0 = \frac{1}{2\sigma\tau}$, where σ is the absorption cross section and τ is the lifetime of the upper level.

The absolute values of the amplitudes versus optical intensity are plotted in Ref. 2. The initial intensity dependence of each harmonic can be obtained by expanding Eq. (1) in powers of (I/I_0):

$$a_1 = -\frac{1}{4}\left(\frac{I}{I_0}\right); \; a_2 = \frac{1}{16}\left(\frac{I}{I_0}\right)^2 \qquad (\alpha << 1) \tag{2}$$

In the low-intensity regime the second-harmonic amplitude is proportional to the square of the absorption cross section. The lineshape of the harmonic spectrum will therefore resemble the square of the fundamental spectrum. The rejection ratio against a more weakly absorbing interferent of considerably greater concentration can be obtained directly from Eq. (1). Consider an interferent having concentration N' in the presence of a species of interest having concentration N. The rejection ratios for detection at the fundamental (r_ω) and second harmonic ($r_{2\omega}$) of the chopping frequency are

$$r_\omega = \frac{Na_1}{N'a'_1}; \; r_{2\omega} = \frac{Na_2}{N'a'_2} \tag{3}$$

where the primed quantities designate the interferent.

The improvement in selectivity with second-harmonic detection can be obtained from either Eq. (1) or Eq. (2). Using the exact expression from Eq. (1) yields

$$\frac{r_{2\omega}}{r_{\omega}} = \frac{\alpha'\left[(1 - \alpha^2)^{1/2} - 1\right]}{\alpha\left[(1 - \alpha'^2)^{1/2} - 1\right]} \approx \frac{\alpha}{\alpha'} \tag{4}$$

The approximation on the right is valid in the regime where α, $\alpha' \ll 1$. When the lifetimes of the species of interest and the interferent are the same, then the improvement in selectivity is given approximately by the ratio of their absorption cross sections. This condition would apply if the lifetimes are dominated by relaxation processes that quench both the interferent and the species of interest with the same efficiency.

In the most common experimental situation, the available laser power is fixed. In this case the maximum in the second-harmonic response has been shown to occur near the intensity $1.4\ I_s$.[2] The second-harmonic response at this intensity is merely four times smaller than the fundamental response and only an order of magnitude smaller than the largest possible fundamental response that would occur under completely "unsaturated" conditions.[2] This apparent loss of sensitivity is of negligible consequence when the major detection limitation is noise associated with a high concentration of a mor linearly absorbing interferent. The enhanced discrimination against linear respondents is expected to yield an improved signal-to-noise (S/N) ratio when saturated-harmonic detection is employed.

The second-harmonic improvement is only slightly modified for operations in the intensity regime of maximum second-harmonic response ($I_0 = 1.4\ I_s$). In this case it can be shown that

$$\frac{r_{2\omega}}{r_{\omega}} \approx 0.6\ \frac{\sigma}{\sigma'} \tag{5}$$

This model of harmonic saturated response is valid for spectrally isolated, homogeneously broadened transitions. It is directly applicable to the optical spectra of heavy atoms under atmospheric-pressure conditions where the Doppler width is a small fraction of the homogeneous pressure-broadened linewidth.

However, harmonic saturated spectroscopy is also applicable to molecular transitions in the infrared spectral region.

A. CASE A: DETECTION OF DIATOMIC AND SMALL POLYATOMIC MOLECULES

Diatomic and small polyatomic species exhibit resolved rotational line structure in their vibrational spectra. Under ambient conditions their lineshape originates from homogeneous pressure broadening. In this case the absorption profile is given by a Lorentzian lineshape $\phi(\nu)$:

$$\phi(\nu - \nu_0) = \frac{\delta\nu_L}{2\pi\left[(\nu - \nu_0)^2 + (\delta\nu_L/2)^2\right]} \tag{6}$$

where $\delta\nu_L$ is the homogeneous linewidth of the transition and ν_0 is the line center frequency.

The harmonic amplitude of the transition is given by Eq. (2). The saturation intensity at any position within the line profile is

$$I_0(\nu) = \frac{N_a h\nu}{2\alpha\phi(\nu - \nu_0)\tau} \tag{7}$$

where N_a is the atmospheric number density at the operating temperature and pressure, and α is the absorption coefficient at the peak of the transition.

The improvement in rejection ratio with second-harmonic detection for a sharply structured, pressure-broadened species of interest against a sharply structured, pressure-broadened interferent is

$$\frac{r_{2w}}{r_w} = \frac{I_0'}{I_0} = \frac{\alpha\phi(\nu - \nu_0)}{\alpha'\phi(\nu - \nu_0')} \tag{8}$$

Discrimination against continuum absorptions and window background is discussed in cases C and D.

B. CASE B: DETECTION OF LARGE POLYATOMIC WITH CONGESTED SPECTRA

The infrared absorption spectra of large polyatomics are often composed of numerous spectrally overlapping transitions associated with several vibrational-band envelopes. This causes the overall absorption profile to

REFERENCES

1. C. K. N. Patel and R. J. Kerl, Appl. Phys. Lett. 30, 578 (1977).

2. R. P. Frueholz and J. A. Gelbwachs, Appl. Opt. 19, 2735 (1980).

3. L. B. Kreuzer, J. Appl. Phys. 42, 2934 (1971).

4. A. Yariv, Quantum Electronics, 2nd ed. (John Wiley and Sons, Inc., New York, 1975) p. 170.

5. G. L. Loper, M. A. O'Neill, and J. A. Gelbwachs, Appl. Opt. 22, 3701 (1983).

6. G. Loper, unpublished results.

7. J. I. Steinfeld, I. Burak, D. G. Sutton, and A. V. Nowak, J. Chem. Phys. 52, 5421 (1969).

complete. The detection of other species, including large polyatomics, is also expected to be improved with harmonic saturated spectroscopy. However, in this case the harmonic spectrum may not be easily predicted from the fundamental spectrum.

The intensities required to achieve optical saturation of these species are in the range of 1 through 100 kW/cm^2. The largest harmonic response is obtained in the vicinity of these intensities. A lower intensity will reduce the harmonic response and thus yield a smaller detection sensitivity. However, the improvement in the rejection ratio against an interferent is not significantly affected by a variation in laser intensity below the saturation intensity. This trade-off in response with available laser intensity may be of little consequence when the present detection limitation is governed by absorption caused by an interferent.

VII. CONCLUSION

The theory of harmonic saturated spectroscopy has been developed for homogeneously and inhomogeneously broadened transitions. Discrimination against the response from a weakly absorbing interferent has been predicted in both cases. Harmonic spectra from SF_6 indicate that both qualitative and quantitative information can be obtained with this technique, with only a small loss of absolute sensitivity.

Attempts to experimentally verify enhanced discrimination against the infrared-continuum absorption of water vapor were not successful, because harmonic distortion in the laser modulation waveform generated a harmonic signal from the linearly absorbing water-vapor continuum which was much larger than the saturated harmonic response signal that originated from SF_6. A successful demonstration of enhanced interference discrimination would require a laser modulation technique having a greatly reduced coefficient of second-harmonic intensity modulation.

Our observation of optical pumping at high laser intensity imposes an additional restriction on the nature of the infrared transitions that can form the basis of a detection scheme employing harmonic saturated spectroscopy. Operations with a large polyatomic must be confined to spectral regions containing the lowest frequency infrared transitions originating from the ground states of the molecules under investigation. Transitions that do not conform to this requirement may exhibit harmonic spectra that vary considerably with laser intensity.

Harmonic saturated spectroscopy is most effective in discriminating against interferents when one observes spectrally isolated homogeneously broadened transitions. The detection of diatomic and small polyatomic molecules is expected to be improved with the harmonic saturated technique. These species possess high absorption coefficients and sufficiently low spectral congestion to permit saturation to be attained and to allow predictions of their harmonic spectra to be made. Species such as HBr, HCl, CO, CO_2, NH_3, CH_4, C_2H_4, and C_2H_2 fall into this category. This list is not intended to be

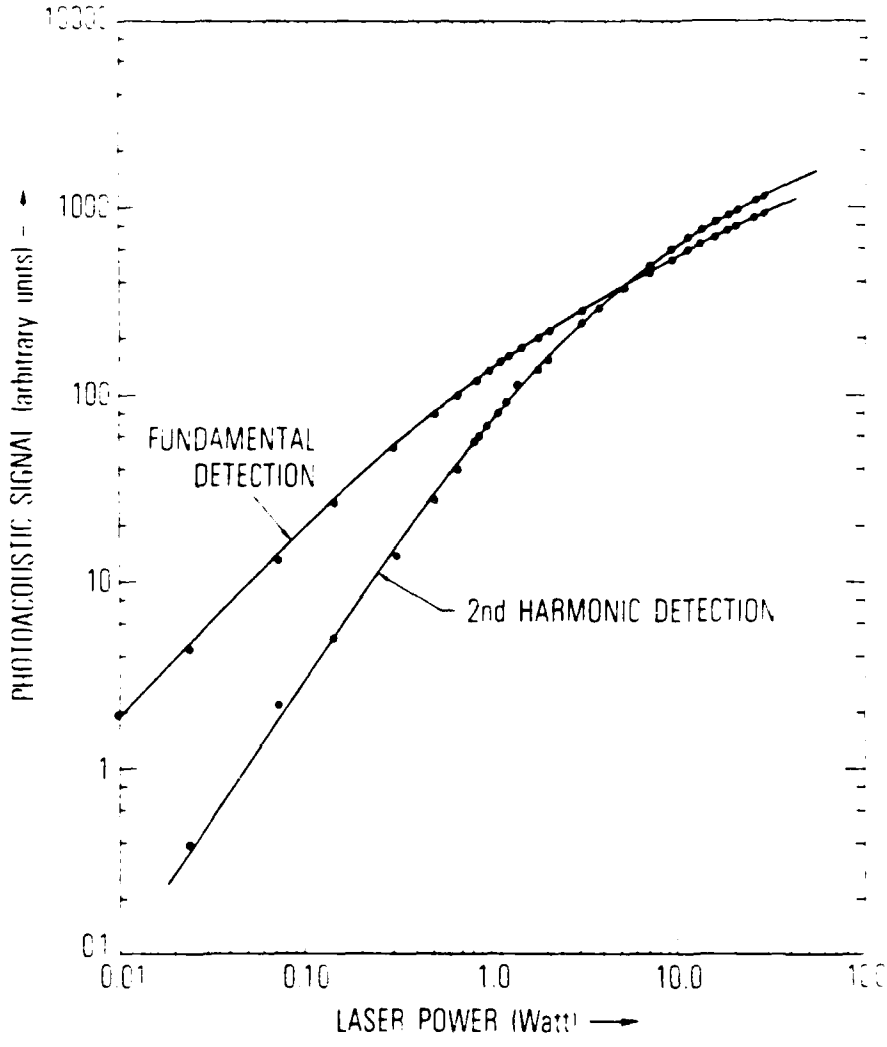

Fig. 3. Dependence of the Fundamental and Harmonic Photoacoustic Responses on the Laser Intensity at f_0 and $2f_0$.

The optical pumping effect results in a transfer of ground-state population into a vibrationally excited mode whose absorption spectrum differs from that of the ground state. It was not possible to deconvolve these high-intensity spectra into their separate harmonic components. Only our measurements at 1 W of excitation power, where the extent of optical pumping is small, could be successfully extracted from the observed signals.

It is also interesting to note from Fig. 2 that the harmonic response at the operating laser intensity was nearly quadratically dependent upon the laser intensity. Notice the dramatic reduction in the halfwidth of the harmonic spectrum relative to that of the fundamental spectrum. This is caused by the quadratic dependence of the harmonic response on the absorption coefficient.

The optical responses at the fundamental and second harmonic of the modulation frequency were obtained as a function of the intensity of the P(16) laser line. The results are plotted in Fig. 3. By means of Eq. (11), the second-harmonic response in the figure has been corrected for the effects of harmonic intensity modulation. The second-harmonic response can be seen to be nearly quadratic with laser intensity, as predicted by the model. At high laser intensity the harmonic response exceeds the fundamental response, because of the nearly order-of-magnitude greater cell response at the harmonic of the modulation frequency.

This information allowed the true saturated harmonic response to be extracted from the measured response by quadrature signal decomposition. The resulting harmonic spectrum, plotted in Fig. 2, was obtained from the following relationship:

$$|S_{2\omega}(\text{true})| = |S_{2\omega}(\text{meas}) - kS_{\omega}(\text{meas})| \qquad (11)$$

where k is a constant having a value that is dependent upon the parameters mentioned above. $S_{\omega}(\text{meas})$ and $S_{2\omega}(\text{meas})$ are the actual signals that were measured at the fundamental and second harmonic of the modulation frequency. Theory predicts that the saturated harmonic signal should have a phase that is π shifted from the phase of the fundamental signal. All of our measurements were performed at the phase that maximized the positive signal response. Since absolute phase measurements were not made, it was not possible to determine the sign of the true harmonic signal. Only the absolute value of the harmonic signal could be determined. It is this quantity, given by Eq. (11), that has been plotted in Fig. 2. We could not absolutely confirm the antiparallel orientation of the fundamental and harmonic signal vectors from our measurements, and were compelled to assume the validity of this predicted behavior in order to generate Eq. (11).

The effects of harmonic distortion in the modulation waveform were expected to become negligible at high laser intensity, where the true harmonic signal strength was anticipated to be much larger than the strength of the background signal induced by harmonic distortion. Attempts to operate in this intensity regime were impeded by the appearance of an additional second-harmonic response produced by optical pumping. This new harmonic signal was shifted in phase relative to the saturated harmonic signal. More extensive quadrature deconvolution is required to decompose the resulting signal into its separate vector components, as follows: (1) the harmonic distortion background response, (2) the true saturated harmonic response, and (3) the optical pumping harmonic response.

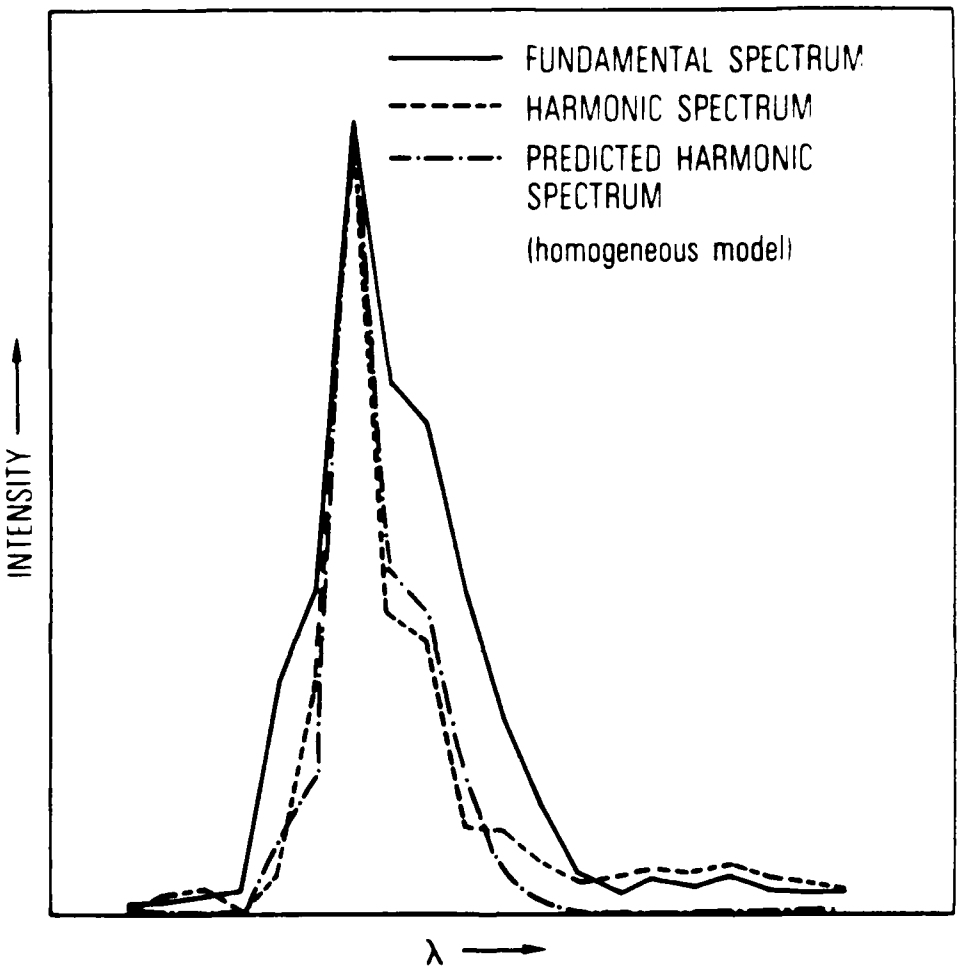

Fig. 2. Fundamental, Harmonic, and Predicted Harmonic Spectra of SF_6. The fundamental spectrum (solid line) is the spectrum that was measured at the modulation frequency. The harmonic spectrum (dashed line) was measured at the second harmonic of the modulation frequency, was corrected for harmonic background distortion, and then was normalized to the peak value of the fundamental spectrum. The predicted harmonic spectrum (dotted and dashed line) is simply the square of the measured fundamental spectrum. It too has been normalized to the peak intensity of the fundamental spectrum.

IV. RESULTS

The solid line in Fig. 2 illustrates the infrared spectrum of SF_6 in the 10-μm regime; the spectrum was obtained at the fundamental modulation frequency with 1 W of power in each discrete emission line of the CO_2 laser. The dashed line in Fig. 2 illustrates the analogous SF_6 spectrum taken at the second harmonic of the modulation frequency. This second-harmonic spectrum has been normalized to the strength of the fundamental signal response at the P(16) laser line. It is actually about 15 times smaller. Furthermore, it is not the direct result of measurements at the harmonic of the modulation frequency. This is because the measured harmonic signal at this laser power contained a large signal contribution originating from laser intensity modulation at the second harmonic of the modulation frequency. The spectrum that we have illustrated by the dashed line in Fig. 2 has been corrected for the harmonic distortion in the laser modulation waveform. This "deconvolution" required the following additional measurements:

1. A determination of the relative amplitudes and phases of the fundamental and second-harmonic components of intensity modulation with the aid of an infrared detector and a lock-in amplifier. The fractional amount of harmonic distortion was found to be 3% of the total intensity modulation under our experimental conditions. The phase at the second harmonic was nearly identical to that at the fundamental when the cross-sectional intensity profile of the laser was adjusted to be as symmetric as possible. All measurements were performed with the most symmetric intensity profile that could be obtained.

2. A measurement of the relative photoacoustic cell responsivities at the fundamental and second harmonic of the modulation frequency. This measurement was performed by filling the cell with a mixture of 20 parts per million of ethylene gas in nitrogen and measuring relative signal amplitudes at the two frequencies in question. The measurement was performed at a laser intensity less than 10 W/cm^2 to insure that the ethylene absorption response was linear and unsaturated. The total amount of absorbed laser energy in this measurement was adjusted to fall within the measured linear response regime of the photoacoustic cell. The cell exhibited a response at the harmonic that was eight times larger than that at the fundamental modulation frequency. This was due to an acoustic resonance at the harmonic of the modulation frequency that was employed to maximize the second-harmonic detector response.

connected to the absorption region by a narrow-bore channel. The linearity of cell response over the dynamic operating range was verified with successively diluted absorbing gas mixtures. At least three decades of linearity were observed in these measurements.

The absolute responsivity of this cell was determined at a frequency of 10 Hz with a dilute mixture of SF_6 and N_2 to be 0.55 V/cm^{-1} W. Under this condition the background response of the cell was measured to be 5 μV/W, corresponding to a background equivalent absorption of 10^{-5} cm^{-1}. The electronic noise with a 15-s time constant was observed to be less than 0.5 μV, corresponding to a theoretical noise equivalent absorptivity of $\sim 10^{-6}$ cm^{-1} W in the absence of background absorption. A background rejection technique would be expected to permit detection of most trace species ($\alpha \sim 10$ cm^{-1} atm^{-1}) in the part-per-billion regime with the available 20 W of laser power.

C. MODULATION WAVEFORM

An approximately sinusoidal waveform was produced with a mechanical chopper (PAR model 192, 60-aperture blade, operated at 400 Hz) that was inserted into a beam-expanded CO_2 laser whose diameter at the point of insertion was equal to the width of the chopper aperture. The second harmonic content of the resulting waveform was measured with an IR sensor and found to vary from 1 through 3%, depending on the symmetry of the laser beam's spatial profile. Geometric chopping converts spatial asymmetry into spatially integrated temporal asymmetry that causes the modulated waveform to contain a small component of second-harmonic intensity modulation.[2] This component generates second-harmonic responses from linearly absorbing species and reduces background discrimination. Minimization of the second-harmonic content of the modulated waveform is essential for the realization of optimum performance. It was not deemed necessary in this preliminary investigation to attempt to achieve this goal. No elaborate measures were adopted to minimize harmonic distortion caused by the spatial mode structure of our laser. Our objective was to verify that a harmonic saturated response could be observed from an infrared molecular transition, and to specify the conditions under which improved detector performance could be realized. In these present experiments, the effects of harmonic distortion could be recognized and deconvolved from the observed data.

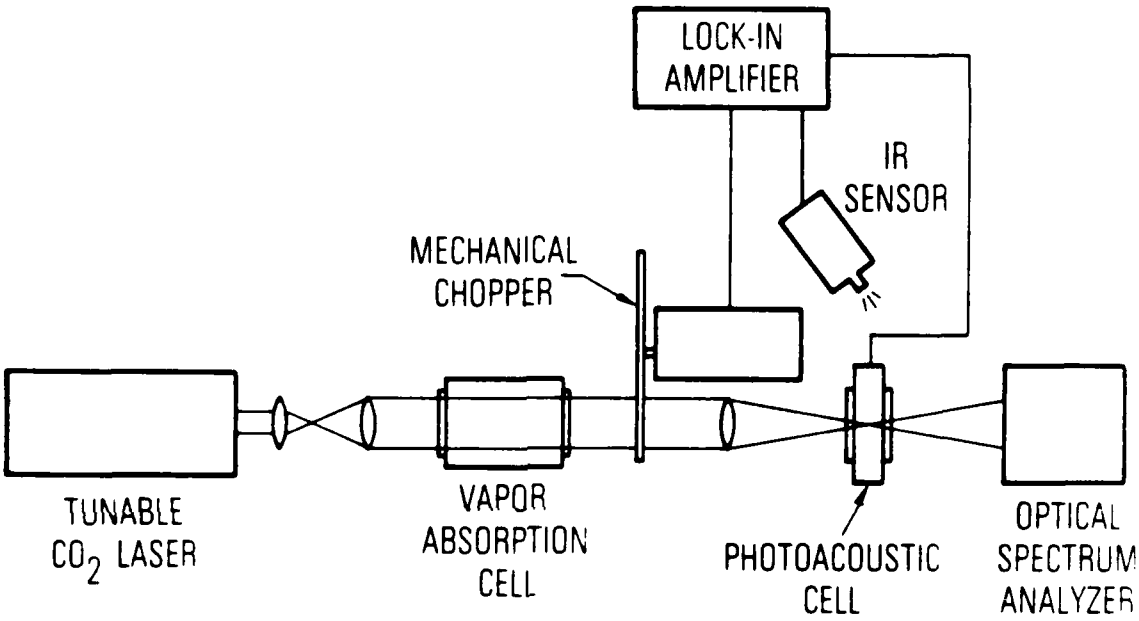

Fig. 1. Schematic Diagram of the Experimental Apparatus. The vapor absorption cell contained SF_6 at a continuously adjustable pressure. It was used to attenuate the laser to the desired intensity. The infrared sensor was used to measure the second-harmonic content of the modulated laser light. The sensor detected scattered laser light originating at the entrance slit of the spectrum analyzer.

III. EXPERIMENTAL PROCEDURES

The experimental apparatus is illustrated in Fig. 1. A description of its various components follows.

A. ABSORPTION GAS AND LASER

A strongly absorbing gas with a characteristic infrared absorption profile spanning several CO_2 laser emission lines was desired for the demonstration of this technique. SF_6 was found to be a suitable candidate, having a strong and broad $\nu_3 \leftarrow 0$ absorption band in the P branch of the 10-μm CO_2 laser band. The peak absorption coefficient at the 10-μm P(16) laser line (948 cm^{-1}) is 686 cm^{-1} atm^{-1} in the presence of one atmosphere of N_2 buffer gas.[6]

Vibrational relaxation in SF_6 under atmospheric conditions proceeds at a rate of 7.14×10^6 s^{-1} from the lowest excited mode,[7] implying a saturation intensity of 2.5 kW/cm^2. This intensity was attained with only moderate focusing of the output from a laboratory-built electric-discharge CO_2 laser. This laser had a 1.8-m cavity length and was operated at pressures of 10 through 25 Torr of laser gas mixture. Tuning was accomplished by manually rotating a 150-groove/mm gold-coated grating and translating a piezoelectrically driven 75% reflecting output coupler. A minimum of 20 W of output power was available from 80 discrete emission lines of this laser. After the beam was expanded to the appropriate dimensions for chopping (see later discussion), it was brought to the desired intensity with a variable attenuation gas-absorption cell (1 through 30 dB), and then focused (f = 5 in.) into the photoacoustic detector. The resulting laser beam diameter was determined to be in the range of 200 through 250 μm. The laser line position, power, and harmonic content were measured as the beam exited the cell.

B. PHOTOACOUSTIC CELL

A miniature cell was constructed to permit attainment of the required saturation intensity over the entire length of the cell. Its path length was 0.5 cm and it had a volume of 1 cm^3. The photoacoustic signal was detected with a Knowles model 1834 electret microphone housed in a chamber that was

of the source of this absorption. Most theories suggest that this absorption is produced by the far wings of strong rotational-vibrational transitions of water vapor molecules or its dimer.[5] These transitions are sufficiently distant from the continuum that they can be considered to be all centered at the same frequency. In this case the continuum absorption would behave almost like that originating from a far wing of a single homogeneous transition. The second-harmonic improvement in rejection ratio would be

$$\frac{r_{2w}}{r_w} = \frac{\alpha\phi(\nu - \nu_0)}{\alpha_{H_2O}(\nu)} \tag{10}$$

where $\alpha_{H_2O}(\nu)$ is the absorption coefficient of water vapor in the continuum region.

Discrimination against other continuum absorption is also possible when detecting polyatomic molecules. In this case the improvement in rejection ratio can only be determined if the complete rotational energy level structure of the manifold is known. In the absence of this knowledge, the following approximate formula can be used:

$$\frac{r_{2w}}{r_w} \approx \frac{\alpha(\nu)}{\alpha_{cont.}(\nu)}$$

where $\alpha(\nu)$ and $\alpha_{cont.}(\nu)$ are the absorption coefficients of the species of interest and the continuum.

D. CASE D: WINDOW ABSORPTION BACKGROUND

The preceding expression can also be used to determine the improvement when the continuum background is produced by an absorption or scattering phenomenon at the cell windows. Background rejection is expected in both cases if the absorption or scattering processes are linear. Window absorption is usually linear since it arises from far-wing continua; scattering is also expected to be linear at the laser intensities in question. Harmonic detection should therefore improve the detectivity of photoacoustic cells that presently exhibit a large window response.

frequency differs from that of the fundamental by the constant factor on the right-hand side of Eq. (9).

Such a model is exactly applicable to a purely inhomogeneously broadened transition, e.g. a Doppler-broadened atomic or molecular transition where the observed lineshape is predominantly determined by a continuous distribution of physically distinguishable translational states. The strict application of this model to a large polyatomic is not valid, because we have ignored the rotational-state dependence of both the transition moments and line center spacings, as well as power broadening of the rotational lineshape. The effective absorption profile of a polyatomic is neither purely homogeneous nor purely inhomogeneous; it lies in an intermediate region between these two extremes. However, both extremes exhibit a harmonic signal strength that depends quadratically on the absorption coefficient. Although we cannot easily predict the exact shape of the harmonic spectrum, we can expect an improvement in rejection ratio with second-harmonic detection. This improvement is given approximately by

$$\frac{r_{2w}}{r_w} \approx \frac{\sigma_v(\nu)}{\sigma_v'(\nu)}$$

where $\sigma_v(\nu)$ and $\sigma_v'(\nu)$ are the integrated vibrational-band strengths of a polyatomic species of interest and a polyatomic interferent. This formula is valid when the absorptions of both species are produced by an inhomogeneous distribution of absorbers. Furthermore, it is only valid near the band center. It predicts no improvement with second-harmonic detection when the vibrational-band strength of the interferent is equal to that of the species of interest.

Discrimination against continuum absorptions and window background is considered next.

C. CASE C: CONTINUUM ABSORPTION BACKGROUND

A discussion of the discrimination capability of saturated harmonic spectroscopy against the water vapor continuum absorption requires knowledge

begin to exhibit inhomogeneous character, because the narrow-linewidth laser radiation interacts with physically distinguishable sets of molecules at atmospheric pressure. These sets are distinguishable because they contain molecules in different rotational and/or vibrational states.

An exact calculation of the harmonic spectrum of a polyatomic molecule could be performed in theory by summing the harmonic contributions from each rotational transition of each vibrational band that contributes to the absorption. Equation (2) can be used to determine the separate rotational contributions, because the simple homogeneously broadened model is valid for the individual rotational transitions. Although such a model may seem intractable, an approximate qualitative solution can be obtained if the rotational transitions within each vibrational band are assumed to be continuously distributed in a uniform fashion. The discrete summation over rotational states can then be approximated by an integration. The amplitudes of the harmonic components become

$$S^{v}_{n\omega}(\nu)d\nu = \int_{-\infty}^{\infty} f(\nu_0)\,[L(\nu - \nu_0)Id\nu]^n d\nu_0 \qquad (n \neq 0)$$

$S^{v}_{n\omega}(\nu)$ is the amplitude of the nth harmonic component that originates from vibrational band v, $f(\nu_0)$ is a factor that governs the distribution of population in the rotational states of the lower vibrational level, $L(\nu - \nu_0)$ is the pressure-broadened homogeneous Lorentzian lineshape of a rotational transition centered at ν_0, and $Id\nu$ is the total laser intensity in bandwidth $d\nu$.

If we assume that $f(\nu_0)$ is constant over the integration region where the Lorentzian factors are dominant,[4] then we obtain the following harmonic amplitude ratio:

$$\frac{S^{v}_{2\omega}(\nu)}{S^{v}_{\omega}(\nu)} = \sigma_v Id\nu \qquad (9)$$

where σ_v is the integrated vibrational-band strength. In this model the profile of the second-harmonic spectrum of an isolated vibrational band is identical to the profile of the fundamental spectrum. Its magnitude at any

LABORATORY OPERATIONS

The Laboratory Operations of The Aerospace Corporation is conducting experimental and theoretical investigations necessary for the evaluation and application of scientific advances to new military space systems. Versatility and flexibility have been developed to a high degree by the laboratory personnel in dealing with the many problems encountered in the nation's rapidly developing space systems. Expertise in the latest scientific developments is vital to the accomplishment of tasks related to these problems. The laboratories that contribute to this research are:

Aerophysics Laboratory: Launch vehicle and reentry fluid mechanics, heat transfer and flight dynamics; chemical and electric propulsion, propellant chemistry, environmental hazards, trace detection; spacecraft structural mechanics, contamination, thermal and structural control; high temperature thermomechanics, gas kinetics and radiation; cw and pulsed laser development including chemical kinetics, spectroscopy, optical resonators, beam control, atmospheric propagation, laser effects and countermeasures.

Chemistry and Physics Laboratory: Atmospheric chemical reactions, atmospheric optics, light scattering, state-specific chemical reactions and radiation transport in rocket plumes, applied laser spectroscopy, laser chemistry, laser optoelectronics, solar cell physics, battery electrochemistry, space vacuum and radiation effects on materials, lubrication and surface phenomena, thermionic emission, photosensitive materials and detectors, atomic frequency standards, and environmental chemistry.

Computer Science Laboratory: Program verification, program translation, performance-sensitive system design, distributed architectures for spaceborne computers, fault-tolerant computer systems, artificial intelligence and microelectronics applications.

Electronics Research Laboratory: Microelectronics, GaAs low noise and power devices, semiconductor lasers, electromagnetic and optical propagation phenomena, quantum electronics, laser communications, lidar, and electro-optics; communication sciences, applied electronics, semiconductor crystal and device physics, radiometric imaging; millimeter wave, microwave technology, and RF systems research.

Materials Sciences Laboratory: Development of new materials: metal matrix composites, polymers, and new forms of carbon; nondestructive evaluation, component failure analysis and reliability; fracture mechanics and stress corrosion; analysis and evaluation of materials at cryogenic and elevated temperatures as well as in space and enemy-induced environments.

Space Sciences Laboratory: Magnetospheric, auroral and cosmic ray physics, wave-particle interactions, magnetospheric plasma waves; atmospheric and ionospheric physics, density and composition of the upper atmosphere, remote sensing using atmospheric radiation; solar physics, infrared astronomy, infrared signature analysis; effects of solar activity, magnetic storms and nuclear explosions on the earth's atmosphere, ionosphere and magnetosphere; effects of electromagnetic and particulate radiations on space systems; space instrumentation.

END

FILMED

8-85

DTIC